

Finite- U induced competing interactions, frustration, and quantum phase transition in a triangular-lattice antiferromagnet

Avinash Singh*

Department of Physics, Indian Institute of Technology Kanpur - 208016

The 120° ordered antiferromagnetic state of the Hubbard model on a triangular lattice presents an interesting case of U -controlled competing interactions and frustration. The spin stiffness is found to vanish at $U \approx 6$ due to competing spin couplings generated at finite U . The loss of magnetic order due to divergent quantum fluctuations yields a magnetic quantum phase transition in the insulating state (at $U \gtrsim 6$). Implications of the quantum spin disordered insulator to the spin-liquid state and Mott transition in the organic systems $\kappa - (\text{BEDT} - \text{TTF})_2\text{X}$ are discussed. Effects of hole and electron doping on magnetic ordering and spin stiffness are also examined.

I. INTRODUCTION

Recent ^1H NMR and static susceptibility measurements on the *nearly isotropic*, triangular-lattice antiferromagnet $\kappa - (\text{BEDT} - \text{TTF})_2\text{Cu}_2(\text{CN})_3$ have shown no indication of long-range magnetic ordering down to 32 mK, well below the estimated exchange constant $J \sim 250$ K, suggesting the realization of a quantum spin-liquid state.¹ No signature of antiferromagnetic (AF) transition was seen in earlier EPR measurements as well.²

On the other hand, a non-collinear 120° ordered ground state is the accepted consensus for the $S = 1/2$ quantum Heisenberg antiferromagnet (QHAF) on an isotropic triangular lattice.^{3,4} Recent quantum Monte Carlo calculations yield a quantum reduction of 59% to the magnetic order from its classical value,⁵ quite close to the spin-wave theory result of 52% at one-loop level,^{6,7} which is somewhat greater than the 40% reduction for the unfrustrated square-lattice.

In this paper we show that the absence of long-range magnetic order in the nearly isotropic organic antiferromagnet $\kappa - (\text{BEDT} - \text{TTF})_2\text{Cu}_2(\text{CN})_3$ can be understood in terms of strongly enhanced quantum spin fluctuations due to finite- U induced competing interactions and frustration, which strongly suppress the spin stiffness in the 120° ordered state. Indeed, for the half-filled Hubbard model on an isotropic triangular lattice, we find that in the insulating ordered state the spin stiffness vanishes at $U_{\text{stiff}}^* \approx 6$. The corresponding divergence in the spin-fluctuation correction implies loss of long-range magnetic order at U_{order}^* which is somewhat higher than U_{stiff}^* , yielding a finite- U magnetic quantum phase transition in the insulating state.

The realization in the triangular lattice of a paramagnetic insulator state at intermediate U , in which magnetic ordering is suppressed by strong quantum spin fluctuations, is interesting as it allows, with decreasing U , for a Mott-type metal-insulator transition not accompanied by any magnetic symmetry breaking. In this context, another quantum correction which assumes significance is that for the AF band gap. Indeed, two different scenarios emerge depending on the relative magnitudes of U_{order}^* and U_{gap}^* , where the 120° AF order and AF band gap vanish, respectively. For $U_{\text{order}}^* > U_{\text{gap}}^*$, more likely for

divergent spin fluctuation due to vanishing spin stiffness, a paramagnetic insulator state lies between the paramagnetic metal (PM) and the AF insulator (AFI), whereas for $U_{\text{gap}}^* > U_{\text{order}}^*$, the magnetic transition is pre-empted, and there is a first-order transition from AFI to PM at U_{gap}^* when the two AF bands start overlapping. Quantum corrections to quasiparticle dispersion and band gap due to motion of an added hole (electron) in the AF background, resulting in strong incoherence due to scrambling of the spin ordering, has been recently studied in detail for the $t - t'$ -Hubbard model on a square lattice.⁸

The divergent quantum spin fluctuations and resulting loss of magnetic order due to vanishing spin stiffness may actually be a precursor to an exotic quantum spin-disordered state, as for the frustrated square-lattice antiferromagnet. Indeed, for the spin-half $J - J'$ Heisenberg model on a square lattice, or equivalently the strong-coupling $t - t'$ Hubbard model, where the frustrating NNN coupling $J' = 4t'^2/U$ leads to vanishing spin stiffness at $J'/J = t'^2/t^2 = 0.5$,⁹ series-expansion study¹⁰ of the ground-state energy indicates a continuous transition from the AF state (which breaks spin-rotation symmetry) to a columnar dimer (valence-bond-solid) state (which breaks lattice translation symmetry) at $J'/J \sim 0.4$, which is surprisingly very close to where the one-loop-level AF order also vanishes.⁹ Recently there has been strong interest in the critical theory of continuous quantum phase transitions between two phases with different broken symmetry, which requires going beyond the Landau-Ginzburg-Wilson paradigm.¹¹

The suppression of magnetic ordering due to enhanced spin fluctuations is therefore also relevant in the layered system $\kappa - (\text{BEDT} - \text{TTF})_2\text{Cu}[\text{N}(\text{CN})_2]\text{Cl}$, which exhibits a genuine Mott transition not accompanied by any symmetry breaking.¹² Generally, the organic systems $\kappa - (\text{BEDT} - \text{TTF})_2\text{X}$, where X denotes inorganic monovalent anion, have emerged as a new class of correlated electron systems exhibiting antiferromagnetism, superconductivity, and metal-insulator transition.^{13,14} Recent discovery of superconductivity in $\text{Na}_x\text{CoO}_2 \cdot y\text{H}_2\text{O}$ ¹⁵ and the observation of low-temperature insulating phases in some $\sqrt{3}$ -adlayer structures such as K on Si[111],¹⁶ have also renewed interest in correlated electron system on triangular lattices. As a recent example of quasi-

two-dimensional antiferromagnetism on a triangular lattice exhibiting the 120° spin ordering, $\text{RbFe}(\text{MoO}_4)_2$ has been studied using elastic neutron scattering,¹⁷ and magnetic resonance and magnetization experiments.¹⁸

The Hubbard model on a triangular lattice has been studied recently using a variety of tools. The non-magnetic insulating state near the Mott transition has been studied using the path integral renormalization group method,¹⁹ in which the HF results are systematically improved to reach the true ground state by taking account of quantum fluctuations. Results show a generic emergence of a non-magnetic insulating state sandwiched by a Mott metal-insulator transition and an AF transition. The zero-temperature phase diagram has been studied using the slave boson technique and the exact diagonalization.²⁰ The mean-field SB approach yields a rich phase diagram qualitatively resembling the HF results.²¹ One-electron density of states has been examined using the quantum Monte Carlo method,²² showing a pseudogap development for intermediate U , accompanied by two peaks in the spin structure factor, signaling the formation of a spiral SDW. A weak-coupling RG analysis applied to the anisotropic triangular lattice shows that frustration suppresses the spin-wave instability in favour of a superconducting instability.²³ A magnetic field induced exotic spin-triplet superconductivity has been proposed having strong ferromagnetic fluctuations.²⁴ Ground-state spin structure of Cr and Mn monolayers on $\text{Cu}[111]$, proposed as ideal candidates for physical realization of frustrated 2D *itinerant* antiferromagnets, has been investigated by performing *ab initio* calculations based on the density-functional theory in the local spin-density approximation.²⁵

We consider the Hubbard model

$$\mathcal{H} = -t \sum_{i,\delta} a_{i,\sigma}^\dagger a_{i+\delta,\sigma} + U \sum_i a_{i\uparrow}^\dagger a_{i\uparrow} a_{i\downarrow}^\dagger a_{i\downarrow} \quad (1)$$

with nearest-neighbour (NN) hopping on a triangular lattice, and focus on the effect of finite- U induced competing interactions on quantum spin fluctuations in the 120° ordered state. The mean-field state is briefly reviewed in section II to introduce the notation. We obtain the spin fluctuation propagator (section III) and study the spin-wave excitations and spin stiffness in the full U range (section IV). We also examine the effects of hole and electron doping on magnetic ordering (section V).

II. MEAN-FIELD STATE

There are two alternative mean-field descriptions of the 120° ordered AF state — i) a spiral-state representation, with an ordering wavevector $\mathbf{Q} = (2\pi/3, 2\pi/\sqrt{3})$, and ii) a three-sublattice representation, involving the local mean fields Δ_α on the three sublattices $\alpha = \text{A, B, C}$. The energy eigenvalues and eigenvectors of the sublattice-basis $[6 \times 6]$ Hamiltonian matrix can be conveniently ob-

tained from those of the spiral-state $[2 \times 2]$ Hamiltonian, as described below.

A. Spiral-state representation

With an order parameter $\Delta_{\mathbf{Q}} = -U \sum_{\mathbf{k}} \langle a_{\mathbf{k}-\mathbf{Q}\downarrow}^\dagger a_{\mathbf{k}\uparrow} \rangle$, representing spin ordering in the x - y plane, the Hubbard Hamiltonian reduces to

$$H_{\text{HF}} = \sum_{\mathbf{k}} (a_{\mathbf{k}\uparrow}^\dagger a_{\mathbf{k}-\mathbf{Q}\downarrow}^\dagger) \begin{bmatrix} \epsilon_{\mathbf{k}} & \Delta_{\mathbf{Q}} \\ \Delta_{\mathbf{Q}}^* & \epsilon_{\mathbf{k}-\mathbf{Q}} \end{bmatrix} \begin{pmatrix} a_{\mathbf{k}\uparrow} \\ a_{\mathbf{k}-\mathbf{Q}\downarrow} \end{pmatrix} \quad (2)$$

at the Hartree-Fock (HF) level, where $\epsilon_{\mathbf{k}} = -2t[\cos k_x + 2 \cos(k_x/2) \cos(k_y\sqrt{3}/2)]$ is the triangular-lattice free-fermion energy. Choosing real $\Delta_{\mathbf{Q}}$, the spiral-state quasi-particle energies $E_{\mathbf{k}}^\pm$ and amplitudes ($u_{\mathbf{k}}$ $v_{\mathbf{k}}$) are given by

$$E_{\mathbf{k}}^\pm = \eta_{\mathbf{k}} \pm \sqrt{\Delta_{\mathbf{Q}}^2 + \xi_{\mathbf{k}}^2} \quad (3)$$

$$u_{\mathbf{k}}^2 = \frac{1}{2} \left(1 \pm \frac{\xi_{\mathbf{k}}}{\sqrt{\Delta_{\mathbf{Q}}^2 + \xi_{\mathbf{k}}^2}} \right) \quad (4)$$

$$v_{\mathbf{k}}^2 = \frac{1}{2} \left(1 \mp \frac{\xi_{\mathbf{k}}}{\sqrt{\Delta_{\mathbf{Q}}^2 + \xi_{\mathbf{k}}^2}} \right)$$

for the upper (+) and lower (−) Hubbard bands, where $\eta_{\mathbf{k}} \equiv (\epsilon_{\mathbf{k}} + \epsilon_{\mathbf{k}-\mathbf{Q}})/2$ and $\xi_{\mathbf{k}} \equiv (\epsilon_{\mathbf{k}} - \epsilon_{\mathbf{k}-\mathbf{Q}})/2$. Self-consistency requires that $\Delta_{\mathbf{Q}} = -U \sum_{\mathbf{k}} v_{\mathbf{k}}^* u_{\mathbf{k}}$, which yields the condition

$$\frac{1}{U} = \sum_{\mathbf{k}} \frac{1}{2\sqrt{\Delta_{\mathbf{Q}}^2 + \xi_{\mathbf{k}}^2}} [\theta(E_F - E_{\mathbf{k}}^-) - \theta(E_F - E_{\mathbf{k}}^+)] \quad (5)$$

in which lower and upper band states contribute with opposite sign.

The spin expectation values $\langle S_i^\mu \rangle = \frac{1}{2} \langle \Psi_i^\dagger \sigma^\mu \Psi_i \rangle$ in the spiral state yield

$$\langle S_i^x \rangle = \frac{1}{2} m_{\mathbf{Q}} \cos \mathbf{Q} \cdot \mathbf{r}_i$$

$$\langle S_i^y \rangle = \frac{1}{2} m_{\mathbf{Q}} \sin \mathbf{Q} \cdot \mathbf{r}_i \quad (6)$$

at lattice site i , in terms of the spiral-state magnetization $m_{\mathbf{Q}} = 2 \sum_{\mathbf{k}} \langle a_{\mathbf{k}-\mathbf{Q}\downarrow}^\dagger a_{\mathbf{k}\uparrow} \rangle$. For $\mathbf{Q} = (2\pi/3, 2\pi/\sqrt{3})$ the spiral twisting of spins generates the 120° ordered AF state on the triangular lattice.

B. Three-sublattice representation

While the spiral-state description applies only to Bravais lattices, the sublattice-basis description applies to Kagomé type non-Bravais lattices as well. In the Hartree-Fock approximation, the Hamiltonian reduces to

$$\mathcal{H}_{\text{HF}} = \sum_i \Psi_i^\dagger [-\sigma \cdot \Delta_i] \Psi_i - t \sum_{i,\delta} \Psi_i^\dagger \mathbf{1} \Psi_{i+\delta}, \quad (7)$$

where the local mean field $\Delta_i = \frac{1}{2}U\langle\Psi_i^\dagger\sigma\Psi_i\rangle$. In general, the 120° AF state is characterized by an ordering plane (normal \hat{n}_1) and a planar direction (\hat{n}_2) with reference to which Δ_i make angles 0° , 120° , and 240° on the three sublattices. A convenient choice is $\hat{n}_1 = \hat{z}$ (spin-ordering in the $x-y$ plane) and $\hat{n}_2 = \hat{x}$, so that Δ_i on the three sublattices $\alpha = A, B, C$ are given by

$$\Delta_\alpha = \Delta\hat{\alpha} \quad (\hat{\alpha} = \hat{a}, \hat{b}, \hat{c}) \quad (8)$$

in terms of the three lattice unit vectors

$$\hat{a} = \hat{x}, \quad \hat{b} = -\frac{1}{2}\hat{x} + \frac{\sqrt{3}}{2}\hat{y}, \quad \hat{c} = -\frac{1}{2}\hat{x} - \frac{\sqrt{3}}{2}\hat{y}. \quad (9)$$

As Δ_i is identical on sites of the same sublattice, Fourier transformation within the sublattice basis yields

$$\mathcal{H}_{\text{HF}} = \sum_{\mathbf{k}} \Psi_{\mathbf{k}}^\dagger \begin{bmatrix} -\sigma \cdot \Delta_A & \delta_{\mathbf{k}} & \delta_{\mathbf{k}}^* \\ \delta_{\mathbf{k}}^* & -\sigma \cdot \Delta_B & \delta_{\mathbf{k}} \\ \delta_{\mathbf{k}} & \delta_{\mathbf{k}}^* & -\sigma \cdot \Delta_C \end{bmatrix} \Psi_{\mathbf{k}}. \quad (10)$$

Here $\Psi_{\mathbf{k}} \equiv (a_{\mathbf{k}\uparrow} a_{\mathbf{k}\downarrow} b_{\mathbf{k}\uparrow} b_{\mathbf{k}\downarrow} c_{\mathbf{k}\uparrow} c_{\mathbf{k}\downarrow})$, where $a_{\mathbf{k}}, b_{\mathbf{k}}, c_{\mathbf{k}}$ are fermion operators defined on the three sublattices A, B, C. Wavevector \mathbf{k} lies within the Magnetic Brillouin Zone (MBZ), corresponding to the three inter-penetrating triangular sublattices (lattice parameter $\sqrt{3}a$). The NN hopping term

$$\delta_{\mathbf{k}} = -t \sum_{\hat{\delta}=\hat{a},\hat{b},\hat{c}} e^{i\mathbf{k}\cdot\hat{\delta}} = -t[e^{ik_x} + 2e^{-ik_x/2} \cos(\sqrt{3}k_y/2)] \quad (11)$$

mixes AB, BC, and CA sublattices, which are connected by the three lattice unit vectors.

The six eigenvalues $E_{\mathbf{k},l}^\pm$ and eigenvectors $|\mathbf{k}^\pm, l\rangle$ of the $[6 \times 6]$ Hamiltonian matrix in Eq. (10), corresponding to upper (+) and lower (−) Hubbard bands, follow from Eqs. (3) and (4) for the spiral-state Hamiltonian. Here $l = 1, 2, 3$ refer to the three branches corresponding to momentum values $\mathbf{k}, \mathbf{k} + \mathbf{Q}, \mathbf{k} - \mathbf{Q}$, respectively, \mathbf{k} being restricted to the MBZ. The amplitude $|\mathbf{k}, l\rangle_\alpha$ involves not only the spin orientation ϕ_α corresponding to sublattice α , but also a relative phase angle $\delta_{\mathbf{Q}}^{l,\alpha}$ associated with the spiral twisting, and is given by

$$|\mathbf{k}, l\rangle_\alpha = \begin{pmatrix} u_{\mathbf{k},l} e^{-i\phi_\alpha} \\ v_{\mathbf{k},l} \end{pmatrix} e^{i\delta_{\mathbf{Q}}^{l,\alpha}} \quad (12)$$

where the planar spin orientations $\phi_\alpha = 0^\circ, 120^\circ, 240^\circ$ for the three sublattices. The spiral phase angle

$$\delta_{\mathbf{Q}}^{l,\alpha} = 0, \pm \mathbf{Q} \cdot \mathbf{R}_{\alpha A} \quad (13)$$

(relative to A) for $l = 1, 2, 3$, where $\mathbf{R}_{\alpha A}$ is the primitive lattice vector connecting sublattices α and A. In view of above structure of state $|\mathbf{k}\rangle$, the self-consistency condition $m_\alpha^\mu = 2\Delta_\alpha^\mu/U = \sum_{\mathbf{k},l} \langle \mathbf{k}, l | \sigma^\mu | \mathbf{k}, l \rangle_\alpha$ retains the same form as in Eq. (5).

III. SPIN FLUCTUATIONS

Associated with the spontaneous symmetry breaking of the continuous spin-rotation symmetry of the Hubbard model, there exist gapless transverse fluctuation modes or Goldstone modes, involving fluctuations locally normal to the symmetry-breaking directions. These low-energy excitations play an important role in determining several important physical properties in ordered systems, such as stability of the mean-field ordered state, quantum corrections to the order parameter and ground-state energy, temperature dependence of the order parameter in three dimensions, and renormalization of electron (hole) spectral function and AF band gap due to fermion-magnon scattering of mobile carriers in the magnetic background.

We consider the time-ordered spin fluctuation propagator, the Fourier transform of which is given in the sublattice basis as

$$[\chi(\mathbf{q}, \omega)]_{\alpha\beta}^{\mu\nu} = i \int dt e^{i\omega(t-t')} \sum_j e^{i\mathbf{q} \cdot (\mathbf{r}_i - \mathbf{r}_j)} \times \langle \Psi_G | T[S_i^\mu(t) S_j^\nu(t')] | \Psi_G \rangle \quad (14)$$

where $\alpha, \beta = A, B, C$ are the sublattice indices and $\mu, \nu = x, y, z$ are the spin indices. At the RPA (bubble-sum) level

$$[\chi(\mathbf{q}, \omega)] = \frac{[\chi^0(\mathbf{q}, \omega)]}{1 - U[\chi^0(\mathbf{q}, \omega)]} \quad (15)$$

where the bare particle-hole propagator $[\chi^0(\mathbf{q}, \omega)]$ is obtained by integrating out the fermions in the broken-symmetry state. For the half-filled, insulating state, the added hole (particle) states lie in the lower (upper) Hubbard band, and we have

$$[\chi^0(\mathbf{q}, \omega)]_{\alpha\beta}^{\mu\nu} = \sum_{\mathbf{k}lm} \frac{\langle \sigma^\mu \rangle_\alpha^{+-} \langle \sigma^\nu \rangle_\beta^{-+*}}{E_{\mathbf{k}-\mathbf{q}}^+ - E_{\mathbf{k}}^- + \omega} + \frac{\langle \sigma^\mu \rangle_\alpha^{+-} \langle \sigma^\nu \rangle_\beta^{+-*}}{E_{\mathbf{k}}^+ - E_{\mathbf{k}-\mathbf{q}}^- - \omega}, \quad (16)$$

where $\langle \sigma^\mu \rangle_\alpha^{+-}$ is short-hand notation for the particle-hole spin matrix element on the α sublattice

$$\langle \sigma^\mu \rangle_\alpha^{+-} \equiv \langle \mathbf{k} - \mathbf{q}^+, m | \sigma^\mu | \mathbf{k}^-, l \rangle_\alpha. \quad (17)$$

The bare particle-hole propagator $[\chi^0(\mathbf{q}, \omega)]_{\alpha,\beta}^{\mu\nu}$ is a $[9 \times 9]$ Hermitian matrix in the three sublattice ($\alpha=A, B, C$) and three spin ($\mu = x, y, z$) basis, the (real) eigenvalues $\lambda_{\mathbf{q}}(\omega)$ and eigenvectors $|\phi_{\mathbf{q}}(\omega)\rangle$ of which contain information regarding the massless transverse fluctuations (spin waves) as well as the massive longitudinal fluctuations along the local ordering direction. Also included are the particle-hole (Stoner) excitations across the band gap, given by the poles of $[\chi^0(\mathbf{q}, \omega)]_{\alpha,\beta}^{\mu\nu}$. In the following, we focus on the spin-wave energies $\omega_{\mathbf{q}}$, which are obtained from the poles $1 - U\lambda_{\mathbf{q}}(\omega_{\mathbf{q}}) = 0$ of Eq. (15).

Evaluating and diagonalizing the $[\chi^0(\mathbf{q}, \omega)]$ matrix for $\mathbf{q}, \omega = 0$, we obtain three Goldstone modes $U\lambda_n = 1$, as expected for the non-collinear 120° AF state, corresponding to rigid spin rotations about the x, y, z axes. Rotation

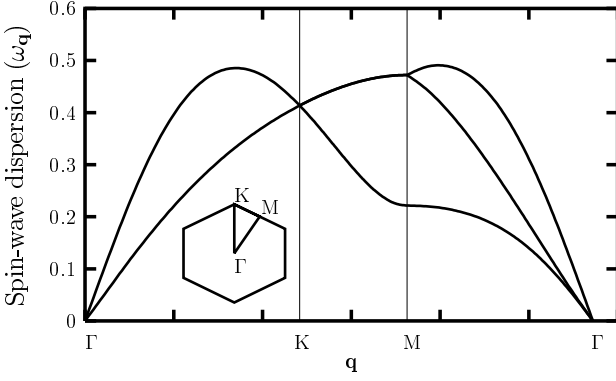


FIG. 1: The spin-wave dispersion along different symmetry directions of the MBZ (inset), for $\Delta = 4$.

around the z axis yields an in-plane mode involving S^x and S^y fluctuations, while those around the x and y axes yield two out-of-plane modes involving only S^z fluctuation. The corresponding eigenvectors, giving transverse fluctuation amplitudes on the three sublattices, are

$$\begin{pmatrix} \hat{y} \\ -\frac{\sqrt{3}}{2}\hat{x} - \frac{1}{2}\hat{y} \\ \frac{\sqrt{3}}{2}\hat{x} - \frac{1}{2}\hat{y} \end{pmatrix}, \begin{pmatrix} 0 \\ \hat{z} \\ -\hat{z} \end{pmatrix} \text{ and } \begin{pmatrix} 1 \\ \frac{1}{2}\hat{z} \\ -\frac{1}{2}\hat{z} \end{pmatrix} \quad (18)$$

For small \mathbf{q}, ω , the Goldstone mode eigenvalue $\lambda_{\mathbf{q}}(\omega)$ has the following typical form for the AF state:

$$\lambda_{\mathbf{q}}(\omega) = \frac{1}{U} - \mathcal{A}q^2 + \mathcal{B}\omega^2, \quad (19)$$

where the coefficient \mathcal{A} of the q^2 term is proportional to the spin stiffness ρ . The pole equation $1 - U\lambda = 0$ yields the spin-wave energy $\omega_{\mathbf{q}} = cq$, where the spin-wave velocity $c = \sqrt{\mathcal{A}/\mathcal{B}} \propto \sqrt{\rho}$ is related to the spin stiffness.

IV. SPIN-WAVE SPECTRUM

The full spin-wave dispersion along different symmetry directions in the Magnetic Brillouin Zone is shown in Fig. 1, for $\Delta = 4$. Along the Γ -K direction, the softer mode is doubly degenerate, and the dispersion continues along the K-M direction after crossing at the MBZ vertex K, where all three modes become degenerate. The degeneracy is resolved along the M- Γ direction, but two modes again become degenerate near Γ , and these represent the two out-of-plane fluctuation modes.

We next consider the spin-wave energy at the MBZ vertices K with $\mathbf{q} = (0, 4\pi/3\sqrt{3})$ etc., where all three spin-wave modes are degenerate, allowing for a convenient comparison with the strong-coupling result. In the strong-coupling limit ($U/t \rightarrow \infty$), the spin-wave energies are given by:

$$\omega_{\mathbf{q}} = 3JS[(1 - \gamma_{\mathbf{q}})(1 + 2\gamma_{\mathbf{q}})]^{1/2} \quad (20)$$

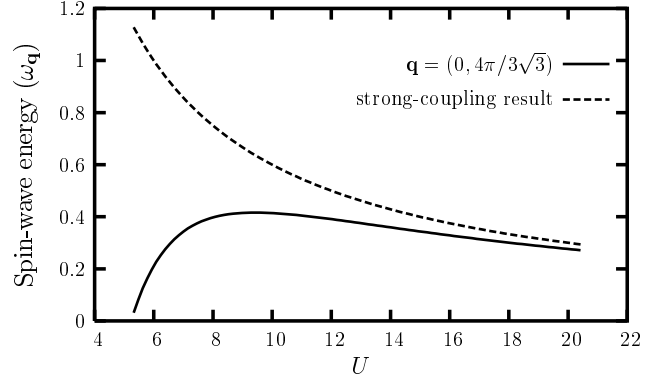


FIG. 2: The spin-wave energy at the Magnetic Brillouin Zone vertices K, along with the strong-coupling result $3JS$.

where $\gamma_{\mathbf{q}} = \frac{1}{3}[\cos q_x + 2\cos(q_x/2)\cos(q_y\sqrt{3}/2)]$, and the three modes correspond to momenta \mathbf{q} , $\mathbf{q} + \mathbf{Q}$, and $\mathbf{q} - \mathbf{Q}$. As $\gamma_{\mathbf{q}} = 0$ for all three modes for $\mathbf{q} = (0, 4\pi/3\sqrt{3})$, the spin-wave modes are three-fold degenerate, with $\omega_{\mathbf{q}} = 3JS = 6t^2/U$ for $S = 1/2$. Figure 2 shows the variation of $\omega_{\mathbf{q}}$ with U , along with the strong-coupling result for comparison. With decreasing U , the spin-wave energy turns over, and the decreasing band gap effectively squeezes the spin-wave spectrum. Indeed, $\omega_{\mathbf{q}}$ vanishes with the gap at $U \approx 5$. This is a typical weak-coupling dynamical effect for an itinerant antiferromagnet.²⁶ The divergence in the eigenvalue $\lambda_{\mathbf{q}}(\omega)$ of the $[\chi^0(\mathbf{q}, \omega)]$ matrix in Eq. (16), when spin-wave energy approaches the charge gap, not only limits the spin-wave spectrum to within the charge gap, but also strongly suppresses the spin-wave amplitude due to wave-function renormalization.

Turning now to long wavelength modes, we consider the two spin-wave velocities ($c = \omega_{\mathbf{q}}/q$) corresponding to in-plane (c_{\parallel}) and out-of-plane (c_{\perp}) fluctuations. For $\mathbf{q} = 0$, the off-diagonal matrix elements of $[\chi^0(\mathbf{q}, \omega)]$, involving in-plane ($\mu = x, y$) and out-of-plane ($\nu = z$) spin indices, vanish identically, implying no mixing between the in-plane mode of the $x - y$ sector and the two out-of-plane modes of the z sector. Mixing is negligible for $q \ll 1$ as well, and therefore small- q spin-wave modes can also be identified in terms of in-plane and two out-of-plane fluctuations. In view of the degeneracy along the $\Gamma - A$ direction, it is convenient to consider $\mathbf{q} = (0, q_y)$, as the two spin-wave energies then readily yield the two spin-wave velocities, as described below in the strong-coupling limit.

For $q_x = 0$, the two modes $\mathbf{q} \pm \mathbf{Q}$ yield identical values: $\gamma_{\mathbf{q}} = -\frac{1}{3}[1/2 + \cos(q_y\sqrt{3}/2)]$, and hence degenerate spin-wave energies from Eq. (20). For small q_y , one obtains $\omega_{\mathbf{q}} = 3JS(\sqrt{3}/2)q_y$ and $3JS(\sqrt{3}/2\sqrt{2})q_y$ for the modes \mathbf{q} and $\mathbf{q} \pm \mathbf{Q}$, respectively, yielding spin-wave velocities $c_{\parallel} = 3JS(\sqrt{3}/2)$ and $c_{\perp} = 3JS(\sqrt{3}/2\sqrt{2})$, which are in the ratio $c_{\parallel}/c_{\perp} = \sqrt{2}$.

Figure 3 shows the two spin-wave velocities in the full

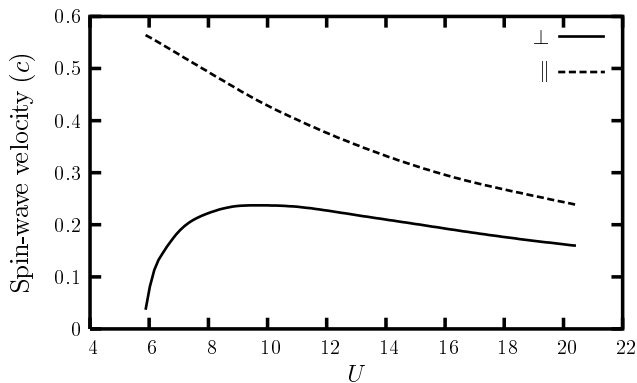


FIG. 3: The spin-wave velocities for in-plane (\parallel) and out-of-plane (\perp) fluctuation modes, showing that c_{\perp} vanishes at $U \approx 6$. The ratio approaches $\sqrt{2}$ in the strong coupling limit.

U range. Both velocities decrease as $1/U$ for large U , and the ratio c_{\parallel}/c_{\perp} asymptotically approaches $\sqrt{2}$ in the strong-coupling limit. The intermediate- U behaviour for the spin-wave velocity corresponding to out-of-plane fluctuations is most interesting, which exhibits a broad peak and falls rapidly with decreasing U , vanishing at a critical interaction strength $U_{\text{stiff}}^* \approx 6$, which is in the insulating regime. For $U < U_{\text{stiff}}^*$, the 120° AF state is therefore unstable with respect to out-of-plane fluctuations.

The vanishing spin-wave velocity and spin stiffness ($\rho_{\perp} \propto c_{\perp}^2$) implies that the one-loop quantum correction to sublattice magnetization due to transverse spin fluctuations diverges. Therefore, the corrected sublattice magnetization will vanish at a critical interaction strength $U_{\text{order}}^* \gtrsim U_{\text{stiff}}^*$, where the quantum reduction exactly eliminates the mean-field order. Hence there is a quantum phase transition in the triangular-lattice AF at $U = U_{\text{order}}^*$ from a 120° ordered state to a spin-disordered state. As described below, this QPT is driven by finite- U induced competing interactions and frustration.

In the strong-coupling limit, the Hubbard model at half filling maps to the $S = 1/2$ QHAF with NN interactions. However, for finite U , extended-range spin couplings (of order t^4/U^3 and higher) are generated, which are all effectively incorporated (at the free-magnon level) within $[\chi^0(\mathbf{q}, \omega)]$, which determines the spin-wave energies. Neglecting dynamical effects, the spin couplings are approximately given by $J_{ij} \approx U^2[\chi^0(\omega = 0)]_{ij}$. Now for the bipartite AF, the next-to-leading $O(t^4/U^3)$ couplings between 2nd neighbours (sites separated by two hoppings) are ferromagnetic, which actually reinforce and stabilize the AF ordering, as seen in the magnetic phase diagram of the $t-t'$ -Hubbard model.⁹ However, the triangular lattice has the peculiarity that several 2nd neighbours are 1st neighbours as well, and the 2nd-neighbour ferromagnetic couplings are therefore a source of additional frustration, leading to spin softening.

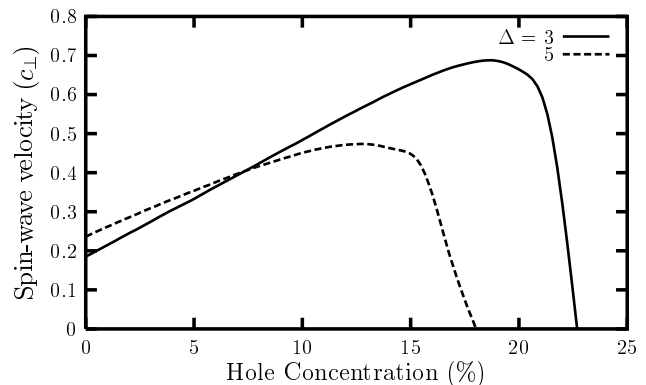


FIG. 4: Doping induced enhancement in spin stiffness of the 120° AF state, as reflected in increasing c_{\perp} with hole doping, is due to additional spin couplings generated by the long-wavelength intraband particle-hole fluctuation processes.

V. HOLE AND ELECTRON DOPING

The two AF bands in the 120° state are quite asymmetrical, with very different Fermi surfaces for hole and electron doping, suggesting quite different behaviour. Indeed, we find that while hole doping stabilizes the AF state and actually increases the spin stiffness, any electron doping destroys AF ordering.

Stability of the square-lattice AF state for hole and electron doping was studied earlier within the $t - t'$ -Hubbard model.²⁷ For finite doping, the Fermi energy lies within a band, and a key role is played by the *in-traband* particle-hole processes in Eq. (16) for $[\chi^0(\mathbf{q}, \omega)]$, which generate additional frustrating spin couplings and affect the stability of the AF state with respect to transverse spin fluctuations. For positive t' , the AF state is destroyed for any hole doping, while a finite concentration is required for electron doping.

We find an even more asymmetric doping behaviour for the triangular lattice. For hole doping in the (broad) lower band in a circular hole pocket around $\mathbf{k} = (0, 0)$, the spin-wave velocity c_{\perp} is seen to significantly *increase* (Fig. 4), reflecting a stabilization of the 120° state due to the extended-range spin couplings generated by the long-wavelength intraband particle-hole processes. With further hole doping, the stiffness rapidly falls to zero, indicating destruction of the AF state.

In contrast, for electron doping in the (narrow) upper band in elliptical electron pockets located symmetrically on the MBZ edges at $\mathbf{k} = \mathbf{Q}/2 = (\pm\pi/3, \pm\pi/\sqrt{3})$ and $(\pm 2\pi/3, 0)$, the maximum transverse response eigenvalue $U\lambda_{\mathbf{q}}$ exceeds 1 (Fig. 5), indicating instability of the 120° AF state. Furthermore, $U\lambda_{\mathbf{q}}$ is seen to be quite independent of the doping concentration, very similar to the square-lattice case for hole doping.²⁷ Also shown for comparison is the transverse response eigenvalue $U\lambda_{\mathbf{q}}$ for hole doping, which further decreases below 1, indicating doping enhanced spin stiffness.

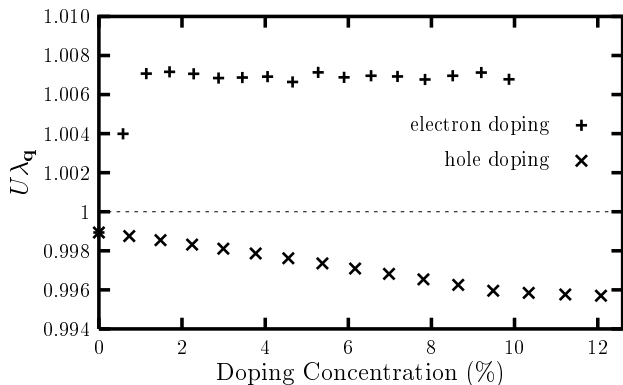


FIG. 5: The maximum transverse response eigenvalue, for $\Delta = 3$, $\mathbf{q} = (0, 0.3)$. The 120° AF state becomes unstable ($U\lambda_{\mathbf{q}} > 1$) for any electron doping, while its stiffness (stability) increases for hole doping.

VI. CONCLUSIONS

In conclusion, spin-wave excitations were studied in the 120° AF state of the Hubbard model on a triangular lattice at half filling as well as for electron and hole doping. The triangular-lattice antiferromagnet presents a novel case of U -controlled competing interactions and frustration, in contrast to the square-lattice case where frustration arises from the NNN coupling generated by the hopping term t' . The spin stiffness was found to vanish at $U \approx 6$, and the divergent quantum spin fluctuation causes a continuous magnetic quantum phase transition at $U_{\text{order}}^* \gtrsim 6$ in the insulating state. The suppression of magnetic ordering due to enhanced quantum spin fluctuations arising from the finite- U induced frustration provides an explanation for why no long-range magnetic ordering is seen in the nearly isotropic triangular-

lattice antiferromagnet $\kappa - (\text{BEDT} - \text{TTF})_2\text{Cu}_2(\text{CN})_3$. Furthermore, the realization of a paramagnetic insulating state at intermediate U , which allows for a first-order paramagnetic metal-insulator transition when the AF band gap vanishes with decreasing U and the two bands begin to overlap, is relevant for the layered system $\kappa - (\text{BEDT} - \text{TTF})_2\text{Cu}[\text{N}(\text{CN})_2]\text{Cl}$, which exhibits a Mott-type metal-insulator transition not accompanied by any magnetic symmetry breaking.

For finite electron and hole doping, when the *intra*band particle-hole processes were incorporated in the spin-fluctuation propagator, the additional spin couplings generated were found to yield a highly asymmetric doping behaviour. While hole doping was found to initially stabilize the AF state and actually increase the spin stiffness, any electron doping was found to destroy the 120° AF ordering. In fact, the instability for electron doping, with nearly concentration independent transverse response eigenvalue $U\lambda_{\mathbf{q}}$, closely resembles the instability of the hole-doped AF on a square lattice.

Finally, whether a paramagnetic insulator intervenes between the paramagnetic metal and the AF insulator depends on the relative strengths of the quantum corrections to magnetic order and AF band gap. In case the AF band gap closes before the magnetic order is lost, the magnetic transition is pre-empted, leaving a first-order AFI - PM transition. In this context, quantum corrections to quasiparticle dispersion and band gap due to motion of an added hole (electron) in the 120° ordered AF background are presently under investigation.

Acknowledgement

Help discussions with Z. Tešanović and V. Ashwin are gratefully acknowledged.

* Electronic address: avinas@iitk.ac.in

- ¹ Y. Shimizu, K. Miyagawa, K. Kanoda, M. Maesato, and G. Saito, Phys. Rev. Lett. **91**, 107001 (2003).
- ² T. Komatsu, N. Matsukawa, T. Inoue, and G. Saito, J. Phys. Soc. Jpn. **65**, 1340 (1996).
- ³ D. A. Huse and V. Elser, Phys. Rev. Lett. **60**, 2531 (1988).
- ⁴ B. Bernu, P. Lecheminant, C. Lhuillier, and L. Pierre, Phys. Rev. B **50**, 10048 (1994).
- ⁵ L. Capriotti, A. E. Trumper, and S. Sorella, Phys. Rev. Lett. **82**, 3899 (1999).
- ⁶ Th. Jolicoeur and J. C. Le Guillou, Phys. Rev. B **40**, 2727 (1989).
- ⁷ A. V. Chubukov, S. Sachdev, and T. Senthil, J. Phys.: Condens. Matter **6**, 8891 (1994).
- ⁸ P. Srivastava and A. Singh, Phys. Rev. B **70**, 115 103 (2004).
- ⁹ A. Singh, cond-mat/0112442 (2001).
- ¹⁰ R. R. P. Singh, Z. Weihong, C. J. Hamer, and J. Oitmaa, Phys. Rev. B **60**, 7278 (1999).

- ¹¹ T. Senthil, S. Balents, S. Sachdev, A. Vishwanath, and M. P. A. Fisher, Phys. Rev. B **70**, 144407 (2004).
- ¹² F. Kagawa *et al.*, Phys. Rev. B **69**, 064 511 (2004); F. Kagawa, T. Itou, K. Miyagawa, and K. Kanoda, cond-mat/0409437 (2004).
- ¹³ K. Kanoda, Physica C **282-287**, 299 (1997); K. Kanoda, Hyperfine Interact. **104**, 235 (1997).
- ¹⁴ R. H. McKenzie, Science, **278**, 820 (1997).
- ¹⁵ K. Takada *et al.*, Nature **422**, 53 (2003).
- ¹⁶ H. H. Weitering, X. Shi, P. D. Johnson, J. Chen, N. J. Dinardo, and S. Kempa, Phys. Rev. Lett. **78**, 1331 (1997).
- ¹⁷ G. Gasparovich, M. Kenzelmann, C. Broholm, L. N. Demianets, and A. Ya. Shapiro, (unpublished).
- ¹⁸ L. E. Svistov, A. I. Smirnov, L. A. Prozorova, O. A. Petrenko, L. N. Demianets, and A. Ya. Shapiro, Phys. Rev. B **67** 094 434 (2003).
- ¹⁹ H. Morita, S. Watanabe, and M. Imada, J. Phys. Soc. Jpn. **71**, 2109 (2002).
- ²⁰ M. Capone, L. Capriotti, F. Becca, and S. Caprara, Phys.

- Rev. B **63**, 085 104 (2001).
- ²¹ H. R. Krishnamurthy, C. Jayaprakash, S. Sarker, and W. Wenzel, Phys. Rev. Lett. **64**, 950 (1990); C. Jayaprakash, H. R. Krishnamurthy, S. Sarker, and W. Wenzel, Europhys. Lett. **15**, 625 (1991).
- ²² M. C. Refolio, J. M. López Sancho, and J. Rubio, cond-mat/0103459 (2001).
- ²³ S.-W. Tsai and J. B. Marston, Can. J. Phys. **79**, 1463 (2001).
- ²⁴ R. Arita, K. Kuroki, and H. Aoki, J. Phys. Soc. Jpn. **73**, 533 (2003).
- ²⁵ Ph. Kurz, G. Bihlmayer, K. Hirai, and S. Blügel, Phys. Rev. Lett. **86**, 1106 (2001).
- ²⁶ P. Sen and A. Singh, Phys. Rev. B **48**, 15792 (1993).
- ²⁷ A. Singh and H. Ghosh, Phys. Rev. B **65**, 134 414 (2002).